Ru doping induced quantum paraelectricity in ferroelectric $Sr_{0.9}Ba_{0.1}TiO_3$

T. Wei,[1] Y. J. Guo,[1] P. W. Wang,[2] D. P. Yu,[2] K. F. Wang,[1,3] C. L. Lu,[1,3] and J.-M. Liu[1,3,a)]
[1]*Nanjing National Laboratory of Microstructure, Nanjing University, Nanjing 210093, People's Republic of China*
[2]*Electron Microscopy Laboratory, Peking University, Beijing 100871, People's Republic of China*
[3]*International Center for Materials Physics, Chinese Academy of Sciences, Shenyang 110016, People's Republic of China*

(Received 21 March 2008; accepted 31 March 2008; published online 2 May 2008)

We investigate the effect of Ru doping on the dielectric and ferroelectric behaviors of polycrystalline $Sr_{0.9}Ba_{0.1}TiO_3$. It is observed that the Ru doping significantly suppresses the ferroelectric mode, as evidenced by the Raman spectroscopy at various temperatures. The enhanced quantum fluctuation associated with the incorporation of Ru^{4+} at *B* site is demonstrated, which transforms $Sr_{0.9}Ba_{0.1}TiO_3$ from the ferroelectric state into a typical quantum paraelectric state. © *2008 American Institute of Physics*. [DOI: 10.1063/1.2913017]

Recently, considerably renewed interests have been focused on $SrTiO_3$ (STO) due to its rich physical properties, such as superconductivity, semiconductivity, incipient ferroelectricity, catalytic activity, and so on. STO is one of the well investigated quantum paraelectrics so far.[1–5] Below temperature $T=105$ K, STO undergoes a phase transition from cubic symmetry ($Pm3m$) to the antiferrodistortive (AFD) teragonal ($I4/mcm$) structure. Upon further cooling, the dielectric permittivity (ε') of STO rapidly increases with decreasing T and subsequently becomes T independent as $T\rightarrow 0$ K. No ferroelectric (FE) transition is detected even though T is down to the lowest limit available so far.[2,3] This effect can be attributed to the large quantum fluctuation (QF) at low T, which essentially suppresses the FE transition and consequently leads to a deviation of $\varepsilon'(T)$ from the Curie–Weiss law and the absence of any dielectric peak.

STO is a typical quantum paraelectric and recently offers a number of attractive new phenomena.[1–5] It is of practical significance to develop various approaches by which the quantum paraelectric state can be replaced by the FE state. Currently, there have been proposed four types of approaches, including the electric field or stress field loading, isotope substitution of oxygen anions, and substitution of Sr cations, so that a FE mode can be activated.[6,7] On the other hand, much attention to the low-T QF in STO has been paid due to the associated fascinating physics. For example, the gigantic photoinduced ε' in quantum paraelectric STO was demonstrated,[4,5] which is tightly related to the QF. Furthermore, direct observation of this fluctuation controlled by the ultraviolet irradiation by means of the T-dependent and photoinduced x-ray absorption spectroscopy spectra at Ti-*K* edge was achieved.[3] In addition, relatively large coupling between magnetism and dielectric properties in quantum FE $EuTiO_3$ was reported.[8]

The substitution of Sr^{2+} by Ba^{2+} in STO can suppress the QF and favor the FE state.[9] The as-produced $Ba_xSr_{1-x}TiO_3$ (BST) was repeatedly investigated because it can be employed in dynamic random access memories or high performance microwave tunable devices.[10] In those cases, the content of Ba is usually high and the room-T dielectric and FE properties were concerned. In this paper, we pay our attention to the low-T property of BST with low Ba content and, in particular, to the effect of Ru doping at *B* site in terms of FE stability, referring to the peculiar band structure of $SrRuO_3$.[11] In detail, we focus on the effect of Ru doping in $Sr_{0.9}Ba_{0.1}TiO_3$ in terms of the quantum fluctuation.

The polycrystalline $Sr_{0.9}Ba_{0.1}Ti_{1-x}Ru_xO_3$ (SBTR) ($x=0$, 0.02, 0.05, and 0.10) samples were synthesized by conventional solid-state reaction. For a comparison, polycrystalline STO sample was prepared. Highly purified powders $SrCO_3$ (99%), $BaCO_3$ (99%), TiO_2 (99.99%), and RuO_2 (99.95%) were mixed in stoichiometric ratios, ground, and then calcined at 1150 °C for 10 h. The resultant powders were reground and pelletized under 20 MPa pressure into disks of 2 cm in diameter and sintered at 1400 °C for 6 h. Gold electrodes were sputtered on sample surfaces for electrical measurements. X-ray diffraction (XRD) with Cu $K\alpha$ radiation at room temperature was used to check the phase and structure. The dielectric property was measured using the HP4294A impedance analyzer by inserting the samples into the Janis closed-cycle refrigerator system (Janis Research Company, Inc., USA). To check the FE stability of the samples at various T, the Raman spectroscopy was undertaken using a Renishaw inVia Raman microscope with an Ar ion laser (514 nm) source. The laser beam was focused by a microscope objective normal to the substrate surface down to a spot size of several microns in diameter. The emitted light was dispersed by a 1800 mm^{-1} grating and detected by a 1/4 in. format charge coupled device with 3.2×2.4 mm^2 slit size. The laser power was kept around 5 mW to avoid thermal effects. The temperature fluctuation due to laser irradiation is ~0.5 K.

Figure 1 gives the XRD spectra for STO and SBTR ($x=0$, 0.02, 0.05, and 0.10). All the samples have single cubic perovskite structures at room T and no secondary phase is found. The sharp diffraction peak indicates excellent crystallinity. Because Ru^{4+} ion has a similar size with Ti^{4+}, no remarkable lattice distortion associated with the doping of Ru^{4+} at Ti site is detected.[12] The lattice constant of SBTR samples is slightly larger than that of STO (0.3905 nm), a reasonable fact because of larger Ba^{2+} ion than Sr^{2+} ion.

Figure 2 displays the variation of ε' with T for all the samples, measured at a frequency $f=100$ kHz of the ac signal. As shown in Fig. 2(a), the $\varepsilon'(T)$ data of STO exhibit the typical quantum paraelectric behavior and no dielectric peak

a)Author to whom correspondence should be addressed. Electronic mail: liujm@nju.edu.cn.

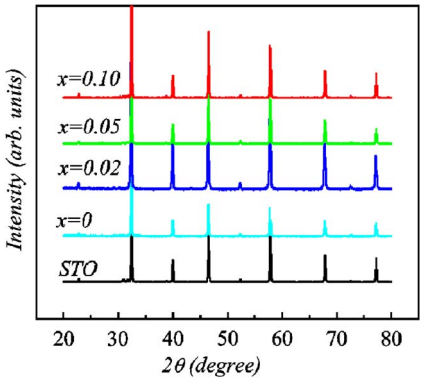

FIG. 1. (Color online) XRD spectra for polycrystalline STO and $Sr_{0.9}Ba_{0.1}Ti_{1-x}Ru_xO_3$ with different Ru doping levels x=0, 0.02, 0.05, and 0.10.

is identified.[2] For the two SBTR samples, x=0 and 0.02, sharp dielectric peaks centered at T=72 and 45 K, respectively, are observed, corresponding to the FE transitions and consistent with earlier experiments.[9] It is seen that the effect of Ru doping is characterized by the left-side shifting Curie temperature T_C, the suppressed peak height $\varepsilon'(T_m)$, and the broadened peak width of the dielectric permittivity ε' as a function of the doping level x, indicating the suppressed FE stability with the doping. We explore the possible mechanisms for this phenomenon below.

Referring to the Ru doping, the suppressed FE state may be ascribed to two aspects. On the one hand, it may be due to the enhanced QF associated with the Ru doping, destabilizing the FE state induced by Ba doping at A site. This picture has been theoretically confirmed from various approaches,[13] and experimentally confirmed for various materials such as $CaTiO_3$, $KTaO_3$, etc. The major feature is that the T-independent dielectric permittivity in low-T limit and a clear plateau of $\varepsilon'(T)$ at $T\rightarrow 0$ K can be identified. The broader this plateau, the more significant the QF.

On the other hand, the suppressed FE transition may be also related to the decreased tetragonal distortion ratio upon the doping of transitional metal with partially filled d orbital, here Ru^{4+} ions, which unfavors the shift of the ions from the center of O_6 octahedra. This mechanism is well established and has been widely employed to explain the exclusion between ferroelectricity and magnetism.[14]

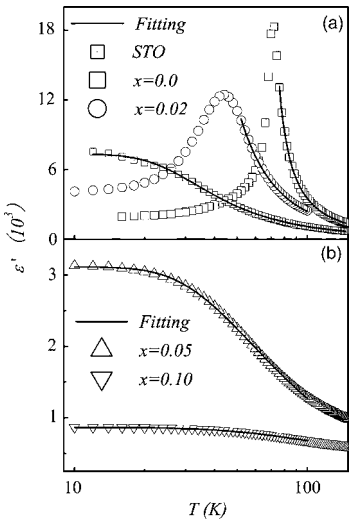

FIG. 2. Measured $\varepsilon'(T)$ data for STO and SBTR with different x=0, 0.02, 0.05, and 0.10. The solid curves are the fitting results using the Barrett equation.

TABLE I. Parameters C, T_1, and T_0 evaluated from fitting of $\varepsilon'(T)$ using Barrett equation.

Samples	C (10^5)	T_1 (K)	T_0 (K)	T_1-2T_0 (K)
STO	0.8	92	35.3	19.4
SBTR x=0.0	1.0	141	89.3	−37.6
SBTR x=0.02	1.15	131	67.7	−4.4
SBTR x=0.05	1.24	101	10.7	79.6
SBTR x=0.10	1.9	94	−172.9	439.8

In order to understand the role of the two possible mechanisms regarding the Ru doping in BST, we perform an additional experiment by increasing the doping level x. The measured $\varepsilon'(T)$ data for SBTR (x=0.05, 0.10) is shown in Fig. 2(b). It is clearly shown that the FE state is completely suppressed and replaced by the typical quantum paraelectric state at the low-T region, characterized by the broad dielectric plateau. In addition, the plateau width at x=0.10 is much broader than that at x=0.05 and x=0.02, indicating the significant QF in these samples. On the other hand, we compare the plateau height ε'_P for the samples of x=0.02, 0.05, and 0.10, and find that it rapidly decreases with increasing x, i.e., $\varepsilon'_P \sim 7500$, 3100, and 900 as x=0.02, 0.05, and 0.10, respectively. This indicates that the Ru doping may also possibly reduce the tetragonal distortion ratio established for SBTR (x=0). At least, the Ru doping does not cause polar clusters which should enhance the dielectric permittivity. Unfortunately, we could not provide direct proof that the suppressed FE state is related to the nonempty d shell of Ru^{4+} which should seek the help from first principle calculation. What should be mentioned here is that the QF induced dielectric plateau is useful for cryogenic applications because the piezoelectric response of the quantum paraelectrics is significant.[15]

To quantitatively understand the QF, we consult the theory on dielectric behavior. The Barrett equation can be used to describe $\varepsilon'(T)$ as[16]

$$\varepsilon' = C/[(T_1/2)\coth(T_1/2T) - T_0], \quad (1)$$

where C is the Curie constant, T_1 represents the tunneling integral, and T_0 is the transition temperature where the lattice instability would occur in the absence of QF. Figures 2(a) and 2(b) also give the excellent fitting (solid lines) of the $\varepsilon'(T)$ data using Eq. (1) and the evaluated parameters, C, T_1, and T_0, are given in Table I.[6] For SBTR, the monotonic decreasing of T_1 and T_0 with increasing x is observed. The negative (T_1-2T_0) is an indication of the FE ordering, while the Ru doping favors the positive (T_1-2T_0), implying the instability of the FE mode due to the QF.[6] The larger the term (T_1-2T_0), the more stable the quantum paraelectric state.[16,17] Therefore, we conclude that the QF is enhanced by the Ru doping and is responsible for the instability of the FE mode in BST.

More convincing evidence with the instability of the FE mode upon Ru doping is given by the Raman spectroscopy. Figure 3 presents the measured Raman spectra for STO and SBTR (x=0 and 0.10) at several Ts. Figure 3(a) shows the entire second-order features for STO with two Raman bands at 200–300 and 600–750 cm^{-1}, respectively. The peaks at

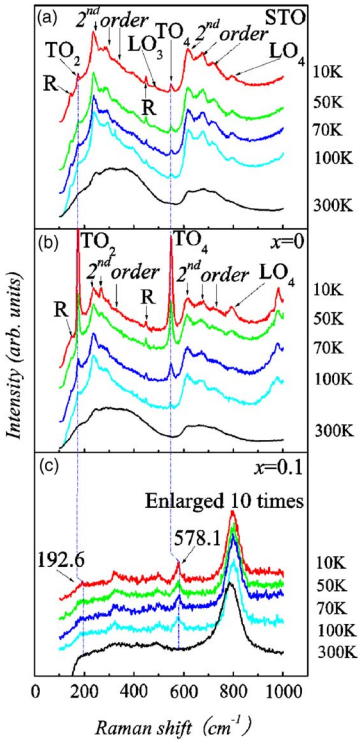

FIG. 3. (Color online) Raman spectra for STO (a) and SBTR ($x=0$) and (b) SBTR ($x=0.10$) at (c) various temperatures ($T=10$, 50, 70, 100, and 300 K).

146 and 446 cm^{-1} originate from the *R* modes corresponding to the AFD transition at 105 K.[18] Figure 3(b) shows the *T*-dependent spectra for SBTR. Strong first-order Raman peaks (single-phonon) can be observed below T_C(72 K). The Raman peaks at 174, 479, 549, and 792 cm^{-1} are the TO_2, TO_4, LO_3, and LO_4 phonons, respectively.[18,19] Furthermore, the intensity of TO_2 and TO_4 phonons considerably decrease with increasing *T* and becomes rather weak above T_C, indicating that the phonons become Raman inactive due to the symmetry selection rules. In fact, TO_2 and TO_4 phonons can be taken as an indicator of the paraferroelectric transition.[18,19]

Figure 4 gives the intensity for the TO_2 and TO_4 phonons as a function of *T* normalized by the Bose factor $n+1=[1-\exp(-h\omega)/2\pi kT]^{-1}$, where *h* is the Planck constant, ω is phonon frequency, and *k* is Boltzmann constant and the intensity of the corresponding mode at $T=10$ K. Both the TO_2 and TO_4 phonons display similar decay trend with increasing T. The solid and dash dot lines are the fittings to the data on the TO_2 and TO_4, respectively. Their intersection with the horizontal axis is taken as T_C, giving $T_C=69$ and 76 K for the TO_2 and TO_4 phonons, respectively.

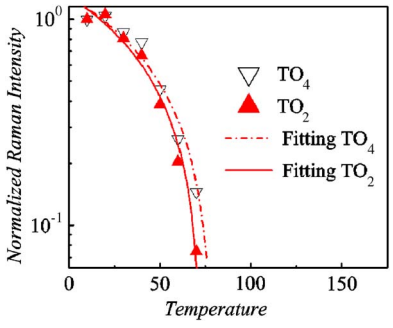

FIG. 4. (Color online) Temperature dependence of Raman intensity for the TO_2 and TO_4 phonons. The solid and dash dot lines are the fitting results.

The Raman spectra for SBTR ($x=0.10$) are given in Fig. 3(c), noting that the detected intensity here is much weaker than those shown in Figs. 3(a) and 3(b). We amplify the intensity by 10 times for clarification. Clearly, the peak shift at 192.6 and 578.1 cm^{-1} with respect to those for SBTR ($x=0$) is attributed to the hardening process of the TO_2 and TO_4 phonons due to the Ru doping at *B* site. Below 100 K, no obvious change of the Raman phonon indicates no FE transition occurring, consistent with our data on the dielectric permittivity presented above. Here, it should be noted that the reason for the weak and broad peak at 800 cm^{-1}, which has nothing to do with the FE mode and QF, is not clearly understood. We argue that this broad peak originates from the photoluminescence for the Raman measurement due to the Ru doping. This issue will be discussed elsewhere.

In conclusion, polycrystalline SBTR ($x=0$, 0.02, 0.05, and 0.10) samples were synthesized and the effect of Ru doping on the FE stability and QF of $Sr_{0.9}Ba_{0.1}TiO_3$ has been investigated. The enhanced QF and broad dielectric plateau at low *T*, as a signature of the quantum paraelectric state associated with the Ru doping at *B* site, have been demonstrated. This work sheds light on modulating the QF in STO-based materials for potential cryogenic piezoelectric applications.

This work was supported by the Natural Science Foundation of China (50601013, 10674061, 50528203) and the National Key Projects for Basic Research of China (2004CB619004, 2006CB921802).

[1] M. Itoh, R. Wang, Y. Inaguma, T. Yamaguchi, Y.-J. Shan, and T. Nakamura, Phys. Rev. Lett. **82**, 3540 (1999).
[2] J. G. Bednorz and K. A. Müller, Phys. Rev. Lett. **52**, 2289 (1984).
[3] S. Nozawa, T. Iwazumi, and H. Osawa, Phys. Rev. B **72**, 121101(R) (2005).
[4] M. Takesada, T. Yagi, M. Itoh, and S. Koshihara, J. Phys. Soc. Jpn. **72**, 37 (2003).
[5] T. Hasegawa, S. Mouri, Y. Yamada, and K. Tanaka, J. Phys. Soc. Jpn. **72**, 41 (2003).
[6] A. Tkach, P. M. Vilarinho, and A. L. Kholkin, Appl. Phys. Lett. **86**, 172902 (2005).
[7] A. Durán, E. Martínez, J. A. Díaz, and J. M. Siqueiros, J. Appl. Phys. **97**, 104109 (2005).
[8] T. Katsufuji and H. Takagi, Phys. Rev. B **64**, 054415 (2001).
[9] V. V. Lemanov, E. P. Smirnova, P. P. Syrnikov, and E. A. Tarakanov, Phys. Rev. B **54**, 3151 (1996).
[10] C. M. Carlson, T. V. Rivkin, P. A. Parilla, J. D. Perkins, D. S. Ginley, A. B. Kozyrev, V. N. Oshadchy, and A. S. Pavlov, Appl. Phys. Lett. **76**, 1920 (2000).
[11] K. Fujioka, J. Okamoto, T. Mizokawa, A. Fujimori, I. Hase, M. Abbate, H. J. Lin, C. T. Chen, Y. Takeda, and M. Takano, Phys. Rev. B **56**, 6380 (1997).
[12] R. D. Shannon, Acta Crystallogr., Sect. A: Cryst. Phys., Diffr., Theor. Gen. Crystallogr. **32**, 751 (1976).
[13] W. Zhong and D. Vanderbilt, Phys. Rev. B **53**, 5047 (1996).
[14] D. I. Khomskii, J. Magn. Magn. Mater. **306**, 1 (2006).
[15] D. E. Grupp and A. M. Goldman, Science **276**, 392 (1997).
[16] J. H. Barrett, Phys. Rev. **86**, 118 (1952).
[17] K. A. Müller and H. Burkhard, Phys. Rev. B **19**, 3593 (1979).
[18] D. A. Tenne, A. Soukiassian, X. X. Xi, H. Choosuwan, R. Guo, and A. S. Bhalla, Phys. Rev. B **70**, 174302 (2004); D. A. Tenne, A. Bruchhausen, N. D. Lanzillotti-Kimura, A. Fainstein, R. S. Katiyar, A. Cantarero, A. Soukiassian, V. Vaithyanathan, J. H. Haeni, W. Tian, D. G. Schlom, K. J. Choi, D. M. Kim, C. B. Eom, H. P. Sun, X. Q. Pan, Y. L. Li, L. Q. Chen, Q. X. Jia, S. M. Nakhmanson, K. M. Rabe, and X. X. Xi, Science **313**, 1614 (2006).
[19] A. B. Shi, W. Z. Shen, and H. Wu, Appl. Phys. Lett. **91**, 112910 (2007).